A DENSITY FUNCTIONAL THEORY STUDY
OF SULFATED MONOLIGNOLS: P-COUMARIL AND CONIFERYL
ALCOHOLS

FERIDE AKMAN,[*] ALEKSANDR S. KAZACHENKO[**,***] and YURIY N. MALYAR[**,***]

[*]*University of Bingöl, Vocational School of Technical Sciences, 12000 Bingöl, Turkey*
[**]*Institute of Chemistry and Chemical Technology SB RAS, Federal Research Center "Krasnoyarsk Science Center SB RAS", Akademgorodok, 50/24, Krasnoyarsk, 660036, Russia*
[***]*Siberian Federal University, Svobodny av., 79, Krasnoyarsk, 660041, Russia*
✉ *Corresponding author: A. S. Kazachenko, leo_lion_leo@mail.ru*

In the present study, sulfated mono- and disubstituted monolignols (p-coumaril, coniferyl alcohols) were investigated by the density functional theory method (DFT/B3LYP) with a 6-311+G (d, p) basis set. New data on these compounds were obtained: optimal configuration, FTIR, ^{1}H and ^{13}C NMR spectra, electronegativity, electrophilicity index, softness HOMO-LUMO analysis and molecular electrostatic potential. The obtained theoretical FTIR and NMR spectra are in good agreement with the experimental data presented in the literature. Based on the results of the study of theoretical ^{13}C NMR spectra, it was shown the introduction of sulfate groups into monolignols shifts the chemical shift towards larger values. According to HOMO-LUMO analysis, the lowest energy gap corresponds to monosulfated coniferyl alcohol. The analysis of the molecular electrostatic potential evidences that the sulfated monolignols contain regions with both nucleophilic reactivity and electrophilic reactivity.

Keywords: density functional theory (DFT), sulfated lignin, monolignols, lignin, sulfated monolignols

INTRODUCTION

Lignocellulosic biomass is a virtually inexhaustible, renewable resource for the production of biofuels and valuable chemicals. Lignin is a natural phenolic macromolecule consisting of three main phenylpropane units, which are derivatives of aromatic alcohols: p-coumaril, coniferyl and synapyl. The lignin content in the lignocellulosic biomass of various plants is from 20 to 30%.[1] In plant cells, lignin functions as a biological barrier and "glue" for binding hemicellulose and cellulose to each other.[2,3]

The existing processes of wood chemical processing are aimed at the production of cellulose, while lignin remains a large-tonnage waste from the pulp and paper and hydrolysis industries,[1] and there are no efficient methods for its utilization.

Lignins (selected in various ways and isolated from various sources) differ in composition and properties.[2] Lignin has a unique structure, which makes it a potential source of valuable products, including aromatic chemicals.[4-6] Despite this, lignin processing technologies are less developed and studied than polysaccharide processing technologies.

A search is currently underway for new, more efficient methods for processing lignins, as well as new areas of their application.[6-8] The production of sulfated lignins is a promising area of lignin utilization. The introduction of a sulfate group in the structure of lignin leads to an increase in its solubility and biodegradability. In addition, sulfated lignin derivatives have antiviral and anticoagulant activity,[9-11] which increases the prospects for their use in pharmaceuticals and medicine. For the sulfation of lignin, various sulfating agents are used (sulfuric and chlorosulfonic acids, oleum, sulfuric anhydride and its complexes with amines),[12,13] and sulfamic acid,[14-16] which is less corrosive; a method of lignin sulfation using enzymes is also known.[17]

The mechanism of the lignin sulfation process by various sulfating agents is diverse. It is known[15,16] that lignin sulfation with sulfamic acid occurs predominantly in aliphatic OH groups, while sulfation with enzymes and sulfur trioxide complexes with organic bases also results in sulfation in aromatic OH groups.[12,13,17]

In the last decade, interest in the study of polymers by theoretical methods has grown significantly.[18,19] These methods are based on calculations of electron circular dichroism (ECD),[20,21] infrared absorption with Fourier transform (FTIR),[22-24] Raman spectroscopy,[18,25,26] nuclear magnetic resonance spectroscopy.[27-32] Theoretical methods make it possible to obtain important properties of a number of polymers.[18,33–35]

The density functional theory (DFT) is an important method of theoretical modeling and it was used to accurately predict the structures, physical and chemical properties of molecules.[32,36]

In this paper, the study of sulfated monolignols by the method of the density functional theory is carried out. Based on published data,[12–17] sulfates of coniferyl and p-coumaryl alcohol were chosen as model compounds, since it is known[15,16] that sulfation is predominantly according to phenyl-propane units (monolignol) in lignin.

EXPERIMENTAL
Theoretical calculations

All theoretical calculations were made using Gaussian 09W program package[37] and GaussView 5.0 molecular visualization program.[38] First, the sulfated monolignols were optimized using the density functional theory (DFT) method, with Becke's three parameter hybrid exchange function combined with the Lee-Yang-Parr correlation functional (B3LYP)[39,40] and 6-311+G (d,p) basis set. Then, the vibration frequencies of the sulfated monolignols were calculated and all positive frequency values showed that sulfated monolignols have correct molecular geometries.

To determine, the energies of HOMO-LUMO orbitals, the Mulliken atomic charges, the NMR and FTIR analysis, the electronic parameters and the MEP analysis were used by using the same method.

RESULTS AND DISCUSSION

It is known[16] that sulfation of lignin with sulfamic acid proceeds via aliphatic OH groups, while sulfation with chlorosulfonic acid and enzymatic sulfation also involves aromatic OH groups[12,17] (Fig. 1).

For understanding the mechanism of lignin sulfation with various reagents, we studied monolignols sulfated in various positions (coniferyl and p-coumaryl alcohol) using the density functional theory method.

The following were used as model compounds of monolignols: sodium monosulfate p-coumarin alcohol (sodium (E)-3-(4-hydroxyphenyl) allyl sulfate), sodium disulfate p-coumarin alcohol (sodium (E)-4-(3-(sulfonatooxy) prop-1-en-1-yl) phenyl sulfate, sodium coniferyl alcohol monosulfate (sodium (E)-3-(4-hydroxy-3-methoxyphenyl) allyl) sulfate and sodium coniferyl alcohol disulfate (sodium (E)-2-methoxy-4-(3-(sulfonatooxy) prop-1-en-1-yl) phenyl sulfate).

Optimized geometry

The optimization of the molecular geometry of sulfated monolignols (sulfated coniferyl and p-coumaryl alcohol) was performed using the 6-311+G (d, p) basis set (Fig. 2).

Optimized geometrical parameters for sulfated p-coumaryl alcohol (Fig. 2 (a) and (b)) and sulfated coniferyl alcohol (Fig. 2 (c) and (d)) are shown in Table 1 and Table 2, respectively.

For a sample of sulfated p-coumaryl alcohol – sodium (E)-3-(4-hydroxyphenyl) allyl sulfate ((a) in Fig. 2 and Table 1), the longest bond lengths are observed for the following atoms: C9-C10 (1.490 Å), C6-C8 (1.467 Å), S12-O13 (1.494 Å), S12-O15 (1.506 Å), O15-Na16 (2.223). Whereas another derivative of p-coumaryl alcohol – sodium (E)-4-(3-(sulfonatooxy) prop-1-en-1-yl) phenyl sulfate ((b) in Fig. 2 and Table 1) has the maximum bond lengths for the atoms: C8-C9 (1.490 Å), O10-S11 (1.677 Å), O14-Na15 (2.238 Å), O16-S17 (1.646 Å), O20-Na21 (2.229 Å). The shortest bond lengths for sodium (E)-3-(4-hydroxyphenyl) allyl sulfate ((a) in Fig. 2 and Table 1) and sodium (E)-4-(3-(sulfonatooxy) prop-1-en-1-yl) phenyl sulfate ((b) in Fig. 2 and Table 1) are observed in O7-H21 (0.962 Å) and C1-H22 (1.083 Å), respectively. Maximum bond angles for p-coumaryl alcohol derivatives – sodium (E)-3-(4-hydroxyphenyl) allyl sulfate and sodium (E)-4-(3-(sulfonatooxy) prop-1-en-1-yl) phenyl sulfate – are observed in C6-C8-C9 (127.856°) and C6-C7-C8 (127.687°), respectively. The smallest bond angles for sodium (E)-3-(4-hydroxyphenyl) allyl sulfate and sodium (E)-4-(3-(sulfonatooxy) prop-1-en-1-yl) phenyl sulfate are observed for S12-O15-Na16 (92.575°) and S17-O20-Na21 (92.569°).
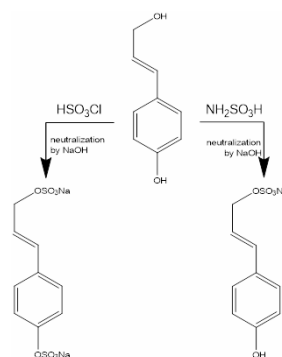
Figure 1: Scheme of lignin sulfation with chlorosulfonic and sulfamic acids (for example, p-coumarin alcohol)
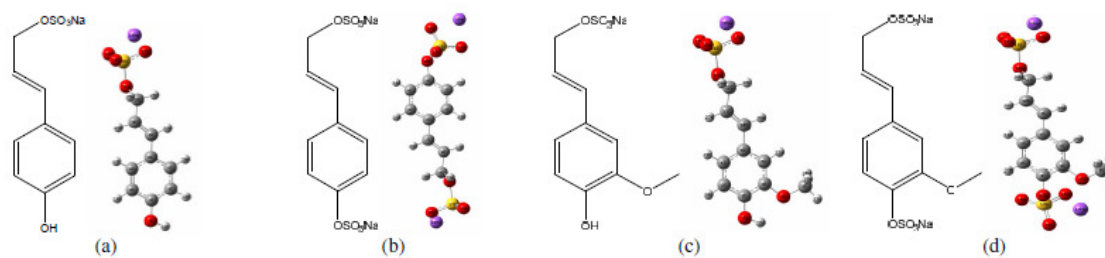

Figure 2: Molecular (left) and optimized (right) structures of sulfated monolignols with atom labelling of (a) sodium (E)-3-(4-hydroxyphenyl)allyl sulfate, (b) sodium (E)-4-(3-(sulfonatooxy)prop-1-en-1-yl) phenyl sulfate, (c) sodium (E)-3-(4-hydroxy-3-methoxyphenyl)allyl sulfate, (d) sodium (E)-2-methoxy-4-(3-(sulfonatooxy)prop-1-en-1-yl) phenyl sulfate

Table 1
Optimized bond lengths (Å) and bond angles (°) of sodium (E)-3-(4-hydroxyphenyl)allyl sulfate (a) and
sodium (E)-4-(3-(sulfonatooxy)prop-1-en-1-yl)phenyl sulfate (b)

Parameters	a	Parameters	b
	Bond lengths (Å)		
C1-C2	1.385	C1-C2	1.388
C1-C6	1.407	C1-C6	1.405
C1-H17	1.083	C1-H22	1.083
C2-C3	1.398	C2-C3	1.395
C2-H18	1.083	C2-H23	1.082
C3-C4	1.393	C3-C4	1.389
C3-O7	1.368	C3-O10	1.392
C4-C5	1.392	C4-C5	1.390
C4-H19	1.086	C4-H24	1.082
C5-C6	1.401	C5-C6	1.403
C5-H20	1.085	C5-H25	1.085
C6-C8	1.467	C6-C7	1.468
O7-H21	0.962	C7-C8	1.338
C8-C9	1.338	C7-H26	1.088
C8-H22	1.089	C8-C9	1.490
C9-C10	1.490	C8-H27	1.086
C9-H23	1.086	C9-O16	1.457
C10-O11	1.457	C9-H28	1.093
C10-H24	1.093	C9-H29	1.094
C10-H25	1.094	O10-S11	1.677
O11-S12	1.647	S11-O12	1.492
S12-O13	1.494	S11-O13	1.450
S12-O14	1.456	S11-O14	1.503
S12-O15	1.506	O14-Na15	2.238
O15-Na16	2.230	O16-S17	1.646
		S17-O18	1.495
		S17-O19	1.456
		S17-O20	1.506
		O20-Na21	2.229
	Bond angles (°)		
C2-C1-C6	121.568	C2-C1-C6	121.505
C2-C1-H17	118.528	C2-C1-H22	118.549
C6-C1-H17	119.904	C6-C1-H22	119.946
C1-C2-C3	119.978	C1-C2-C3	119.298
C1-C2-H18	121.102	C1-C2-H23	120.969
C3-C2-H18	118.919	C3-C2-H23	119.728
C2-C3-C4	119.685	C2-C3-C4	120.659
C2-C3-O7	117.380	C2-C3-O10	122.432
C4-C3-O7	122.936	C4-C3-O10	116.810
C3-C4-C5	119.705	C3-C4-C5	119.345
C3-C4-H19	120.208	C3-C4-H24	119.172
C5-C4-H19	120.087	C5-C4-H24	121.483
C4-C5-C6	121.760	C4-C5-C6	121.525
C4-C5-H20	118.991	C4-C5-H25	119.208
C6-C5-H20	119.249	C6-C5-H25	119.266
C1-C6-C5	117.304	C1-C6-C5	117.654
C1-C6-C8	123.546	C1-C6-C7	123.358
C5-C6-C8	119.150	C5-C6-C7	118.981
C3-O7-H21	109.816	C6-C7-C8	127.687
C6-C8-C9	127.856	C6-C7-H26	114.659
C6-C8-H22	114.572	C8-C7-H26	117.655
C9-C8-H22	117.570	C7-C8-C9	123.228
C8-C9-C10	123.199	C7-C8-H27	121.373

C8-C9-H23	121.437	C9-C8-H27	115.394
C10-C9-H23	115.358	C8-C9-O16	107.327
C9-C10-O11	107.306	C8-C9-H28	111.693
C9-C10-H24	111.597	C8-C9-H29	111.363
C9-C10-H25	111.475	O16-C9-H28	109.199
O11-C10-H24	109.309	O16-C9-H29	108.004
O11-C10-H25	107.937	H28-C9-H29	109.152
H24-C10-H25	109.117	C3-O10-S11	120.522
C10-O11-S12	116.427	O10-S11-O12	100.402
O11-S12-O13	101.673	O10-S11-O13	107.755
O11-S12-O14	107.877	O10-S11-O14	105.179
O11-S12-O15	105.515	O12-S11-O13	117.523
O13-S12-O14	116.934	O12-S11-O14	108.276
O13-S12-O15	108.255	O13-S11-O14	115.852
O14-S12-O15	115.124	S11-O14-Na15	92.726
S12-O15-Na16	92.575	C9-O16-S17	116.393
		O16-S17-O18	101.659
		O16-S17-O19	107.942
		O16-S17-O20	105.538
		O18-S17-O19	116.889
		O18-S17-O20	108.267
		O19-S17-O20	115.096
		S17-O20-Na21	92.569

The longest bond lengths for the sample of sulfated coniferyl alcohol – sodium (E)-3-(4-hydroxy-3-methoxyphenyl) allyl sulfate ((c) in Fig. 2 and Table 2) are observed for the following atoms: C6-C10 (1.468 E), O13-S14 (1.646 E), S14-O15 (1.494 E), S14-O16 (1.506 E), O17-Na18 (2.231). At the same time, for sodium (E)-2-methoxy-4-(3-(sulfonatooxy)   prop-1-en-1-yl) phenyl sulfate ((d) in Fig. 2 and Table 2), the longest bond lengths are observed for the atoms: C10-C11 (1.491 Å), O12-S13 (1.802 Å), O16-Na17 (2.514 Å), O18-S19 (1.649 Å), O22-Na23 (2.237 Å). The minimum bond lengths for sodium (E)-3-(4-hydroxy-3-methoxyphenyl) allyl sulfate ((c) in Fig. 2 and Table 2) and sodium (E)-2-methoxy-4-(3-(sulfonatooxy)   prop-1-en-1-yl) phenyl sulfate ((d) in Fig. 2 and Table 2) are observed in O7-H22 (0.966 Å) and C2-H25 (1.082 Å), respectively. Maximum bond angles for coniferyl derivatives – sodium (E)-3-(4-hydroxy-3-methoxyphenyl) allyl sulfate and sodium (E)-2-methoxy-4-(3-(sulfonatooxy)prop-1-en-1-yl) phenyl sulfate – are observed in C6-C10-C11 (127.851°) and C6-C9-C10 (127.288°), respectively. Minimum bond angles for sodium (E) -3- (4-hydroxy-3-methoxyphenyl) allyl sulfate and sodium (E) -2-methoxy-4- (3- (sulfonatooxy) prop-1-en-1-yl) phenyl sulfate are observed in S14-O17-Na18 (92.546°) and S19-O22-Na23 (92.475°).

Table 2
Optimized bond lengths (Å) and bond angles (°) of (E)-3-(4-hydroxy-3-methoxyphenyl)allyl sulfate (c)
and sodium (E)-2-methoxy-4-(3-(sulfonatooxy)prop-1-en-1-yl)phenyl sulfate (d)

Parameters	c	Parameters	d
Bond lengths (Å)			
C1-C2	1.390	C1-C2	1.388
C1-C6	1.401	C1-C6	1.401
C1-H19	1.082	C1-H24	1.082
C2-C3	1.389	C2-C3	1.392
C2-H20	1.083	C2-H25	1.082
C3-C4	1.404	C3-C4	1.404
C3-O7	1.361	C3-O12	1.368
C4-C5	1.388	C4-C5	1.389

C4-O8	1.374	C4-O7	1.391
C5-C6	1.408	C5-C6	1.406
C5-H21	1.083	C5-H26	1.082
C6-C10	1.468	C6-C9	1.469
O7-H22	0.966	O7-C8	1.429
O8-C9	1.422	C8-H27	1.090
C9-H23	1.088	C8-H28	1.093
C9-H24	1.094	C8-H29	1.093
C9-H25	1.094	C9-C10	1.337
C10-C11	1.338	C9-H30	1.088
C10-H26	1.089	C10-C11	1.491
C11-C12	1.490	C10-H31	1.086
C11-H27	1.085	C11-O18	1.453
C12-O13	1.457	C11-H32	1.094
C12-H28	1.093	C11-H33	1.094
C12-H29	1.094	O12-S13	1.802
O13-S14	1.646	S13-O14	1.478
S14-O15	1.494	S13-O15	1.449
S14-O16	1.456	S13-O16	1.480
S14-O17	1.506	O16-Na17	2.514
O17-Na18	2.231	O18-S19	1.649
		S19-O20	1.494
		S19-O21	1.455
		S19-O22	1.505
		O22-Na23	2.237
Bond angles (°)			
C2-C1-C6	121.096	C2-C1-C6	120.767
C2-C1-H19	118.759	C2-C1-H24	119.043
C6-C1-H19	120.144	C6-C1-H24	120.189
C1-C2-C3	120.378	C1-C2-C3	120.676
C1-C2-H20	121.105	C1-C2-H25	121.215
C3-C2-H20	118.517	C3-C2-H25	118.106
C2-C3-C4	119.359	C2-C3-C4	119.249
C2-C3-O7	120.170	C2-C3-O12	121.970
C4-C3-O7	120.471	C4-C3-O12	118.738
C3-C4-C5	120.156	C3-C4-C5	119.961
C3-C4-O8	113.881	C3-C4-O7	116.415
C5-C4-O8	125.963	C5-C4-O7	123.623
C4-C5-C6	120.899	C4-C5-C6	121.000
C4-C5-H21	120.171	C4-C5-H26	120.583
C6-C5-H21	118.929	C6-C5-H26	118.417
C1-C6-C5	118.112	C1-C6-C5	118.339
C1-C6-C10	123.528	C1-C6-C9	123.347
C5-C6-C10	118.360	C5-C6-C9	118.313
C3-O7-H22	107.792	C4-O7-C8	117.526
C4-O8-C9	118.652	O7-C8-H27	106.381
O8-C9-H23	106.014	O7-C8-H28	111.149
O8-C9-H24	111.093	O7-C8-H29	110.964
O8-C9-H25	111.117	H27-C8-H28	109.246
H23-C9-H24	109.456	H27-C8-H29	109.081
H23-C9-H25	109.455	H28-C8-H29	109.926
H24-C9-H25	109.629	C6-C9-C10	127.288
C6-C10-C11	127.851	C6-C9-H30	114.953
C6-C10-H26	114.709	C10-C9-H30	117.753
C11-C10-H26	117.439	C9-C10-C11	123.341
C10-C11-C12	123.208	C9-C10-H31	121.322
C10-C11-H27	121.396	C11-C10-H31	115.320
C12-C11-H27	115.391	C10-C11-O18	107.099
C11-C12-O13	107.299	C10-C11-H32	111.584

C11-C12-H28	111.641	C10-C11-H33	111.413
C11-C12-H29	111.508	O18-C11-H32	109.590
O13-C12-H28	109.252	O18-C11-H33	108.043
O13-C12-H29	107.909	H32-C11-H33	109.025
H28-C12-H29	109.127	C3-O12-S13	119.844
C12-O13-S14	116.408	O12-S13-O14	95.3313
O13-S14-O15	101.723	O12-S13-O15	107.011
O13-S14-O16	107.898	O12-S13-O16	100.003
O13-S14-O17	105.539	O14-S13-O15	119.022
O15-S14-O16	116.905	O14-S13-O16	112.078
O15-S14-O17	108.234	O15-S13-O16	118.305
O16-S14-O17	115.096	S13-O16-Na17	78.7938
S14-O17-Na18	92.546	C11-O18-S19	116.385
		O18-S19-O20	101.647
		O18-S19-O21	107.709
		O18-S19-O22	105.401
		O20-S19-O21	117.054
		O20-S19-O22	108.289
		O21-S19-O22	115.226
		S19-O22-Na23	92.475

FTIR analysis

For sulfated derivatives of p-coumaryl and coniferyl alcohol, theoretical IR spectra were calculated using the density functional theory method with the 6-311+G (d, p) basis set (Fig. 3).

In the theoretical FTIR spectra for all the samples of sulfated derivatives of monolignols, stretching vibrations of aromatic C-H groups in the region of 3206-3163 cm^{-1} are observed.

Stretching vibrations of OH groups are observed for sodium (E)-3-(4-hydroxyphenyl) allyl sulfate and sodium (E)-3-(4-hydroxy-3-methoxyphenyl) allyl sulfate samples at 3833 and 3777 cm^{-1}. The stretching vibrations of the =C-H group, according to the theoretical FTIR spectra, are in the vicinity of 3158-3118 cm^{-1}. The stretching vibrations of the C=C in the vinyl group of sulfated derivatives of monolignols, according to the theoretical FTIR spectra, are in the vicinity of 1708 cm^{-1}. The calculated aromatic stretching vibrations of the C=C group for sulfated derivatives of monolignols were found in the region of 1403-1650 cm^{-1}.

All the samples of sulfated monolignol derivatives have absorption bands corresponding to the vibrations of sulfate groups at 1254-1277, 1090-1098, 946-992 and 749-754 cm^{-1}.

The stretched values of stretching vibrations correspond to the experimental values presented in the literature.[14-17]
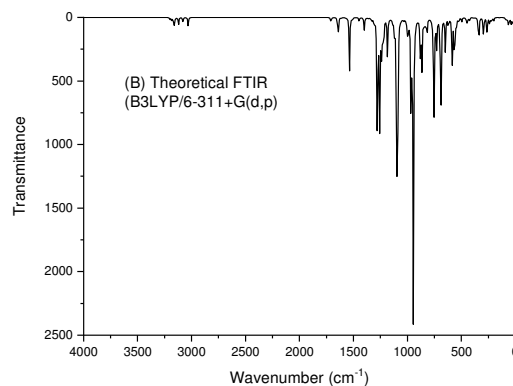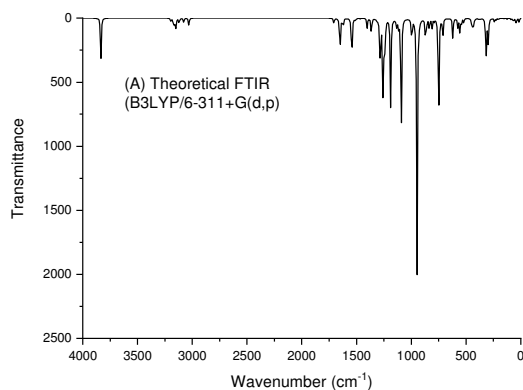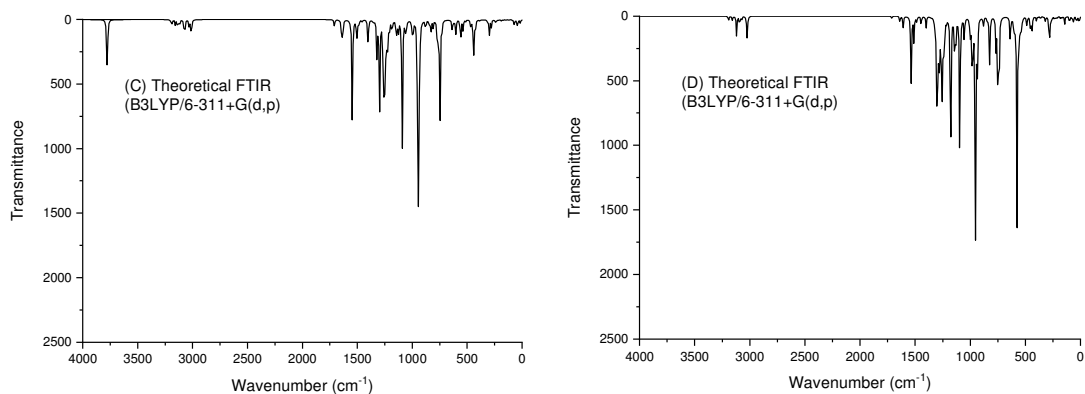
Figure 3: Theoretical FTIR spectra of (A) sodium (E)-3-(4-hydroxy-3-methoxyphenyl)allyl sulfate, (B) sodium (E)-2-methoxy-4-(3-(sulfonatooxy)prop-1-en-1-yl)phenyl sulfate, (C) sodium (E)-3-(4-hydroxy-3-methoxyphenyl)allyl sulfate and (D) sodium (E)-2-methoxy-4-(3-(sulfonatooxy)prop-1-en-1-yl)phenyl sulfate

NMR analysis

The theoretical ^{1}H-NMR spectra of sulfated monolignols are shown in Figure 4. The theoretical ^{1}H-NMR spectra of sulfated monolignol derivatives show characteristic signals at 6.43-7.63 ppm. which are assigned to the protons of the aromatic ring, respectively (Fig. 4, Table 3).

Signals at 4.25 and 3.80 ppm are attributed to the –OH protons bound to the aromatic ring in sodium (E)-3-(4-hydroxy-3-methoxyphenyl) allyl sulfate and sodium (E)-3-(4-hydroxy-3-methoxyphenyl) allyl sulfate samples, respectively.
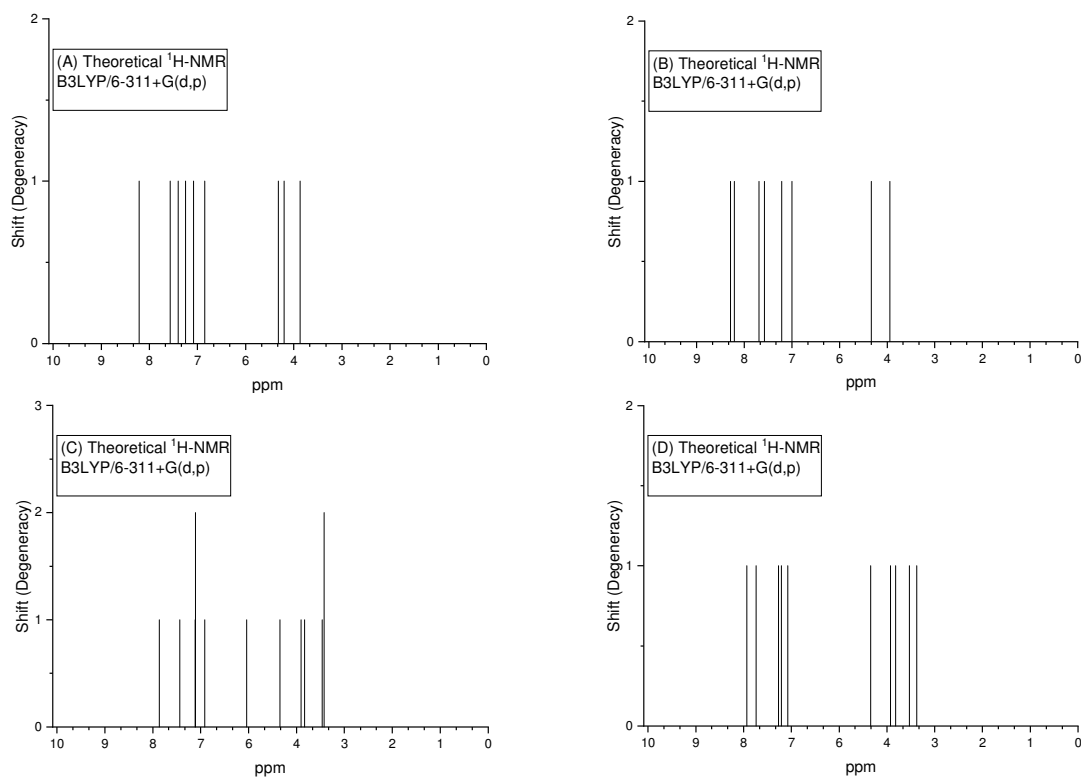

Figure 4: Theoretical ^{1}H-NMR spectra of (A) sodium (E)-3-(4-hydroxy-3-methoxyphenyl)allyl sulfate, (B) sodium (E)-2-methoxy-4-(3-(sulfonatooxy)prop-1-en-1-yl)phenyl sulfate, (C) sodium (E)-3-(4-hydroxy-3-methoxyphenyl)allyl sulfate and (D) sodium (E)-2-methoxy-4-(3-(sulfonatooxy)prop-1-en-1-yl)phenyl sulfate

Figure 5: Theoretical ^{13}C-NMR spectra of (A) sodium (E)-3-(4-hydroxy-3-methoxyphenyl)allyl sulfate, (b) sodium (E)-2-methoxy-4-(3-(sulfonatooxy)prop-1-en-1-yl)phenyl sulfate, (c) sodium (E)-3-(4-hydroxy-3-methoxyphenyl)allyl sulfate and (d) sodium (E)-2-methoxy-4-(3-(sulfonatooxy)prop-1-en-1-yl)phenyl sulfate
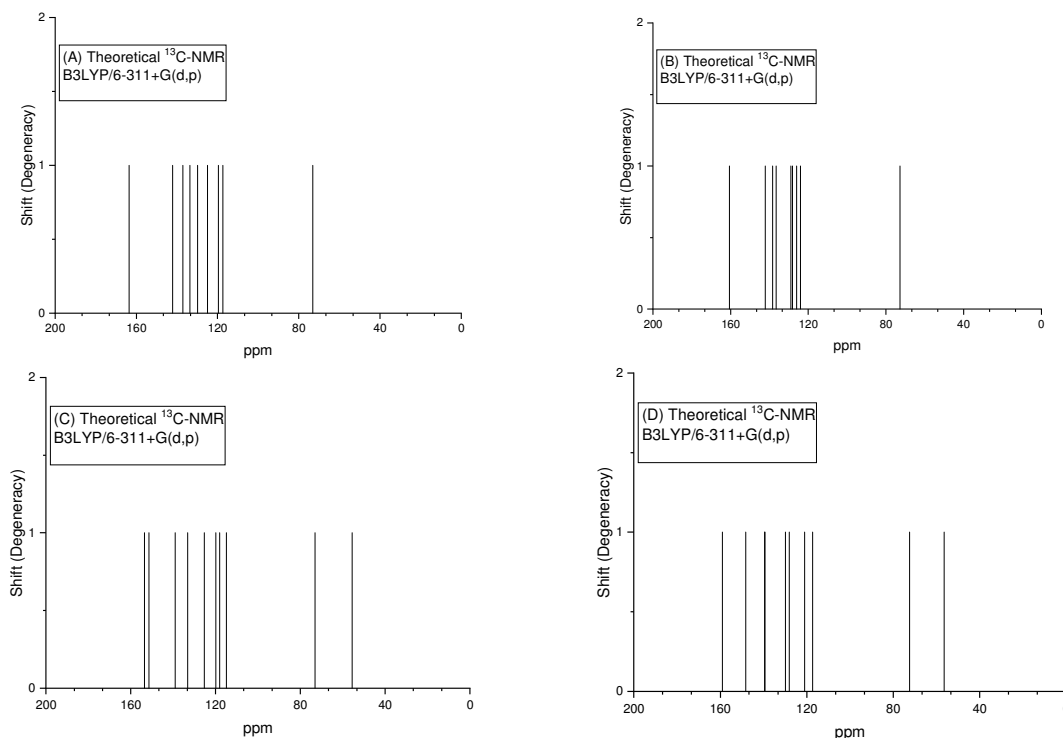
Table 3

Chemical shifts of (a) sodium (E)-3-(4-hydroxy-3-methoxyphenyl)allyl sulfate, (b) sodium (E)-2-methoxy-4-(3-(sulfonatooxy)prop-1-en-1-yl)phenyl sulfate, (c) sodium (E)-3-(4-hydroxy-3-methoxyphenyl)allyl sulfate and (d) sodium (E)-2-methoxy-4-(3-(sulfonatooxy)prop-1-en-1-yl)phenyl sulfate

a		b		c		d	
Atoms	Chemical shifts	Atoms	Chemical shifts	Atoms	Chemical shifts	Atoms	Chemical shifts
17-H	7.93	22-H	8.02	19-H	7.55	24-H	7.63
20-H	7.22	23-H	7.92	20-H	7.07	25-H	7.41
18-H	7.04	25-H	7.35	21-H	6.72	26-H	6.89
19-H	6.87	24-H	7.23	26-H	6.72	30-H	6.82
22-H	6.69	26-H	6.83	27-H	6.50	31-H	6.68
23-H	6.43	27-H	6.60	22-H	5.54	33-H	4.77
25-H	4.75	29-H	4.76	29-H	4.77	32-H	4.31
21-H	4.62	28-H	4.33	28-H	4.29	27-H	4.19
24-H	4.25	3-C	160.66	23-H	4.21	28-H	3.88
3-C	163.61	7-C	142.23	24-H	3.80	29-H	3.71
8-C	142.17	6-C	138.28	25-H	3.76	4-C	158.99
5-C	137.07	5-C	136.61	3-C	153.52	3-C	148.25
6-C	133.63	1-C	128.97	4-C	151.44	9-C	139.44
1-C	129.88	8-C	128.11	10-C	139.02	6-C	139.32
9-C	124.95	4-C	125.94	6-C	133.20	10-C	129.87
2-C	119.52	2-C	123.97	11-C	125.24	2-C	128.14
4-C	117.42	9-C	72.79	1-C	119.78	1-C	120.94
10-C	73.11	21-Na	587.79	2-C	118.11	5-C	117.29
16-Na	587.94	15-Na	589.48	5-C	114.89	11-C	72.42
				12-C	73.11	8-C	56.46
				9-C	55.57	17-Na	585.26
				18-Na	588.072	23-Na	588.67

In sulfated derivatives of p-coumaril alcohol, the signals at 4.75-4.76 ppm are attributed to –CH$_2$ protons adjacent to ethylene and hydroxyl groups. Signals between 8.02 and 7.04 ppm usually attributed to the chemical shift of protons in the aromatic ring. The introduction of an additional sulfate group into the p-coumaryl alcohol structure leads to a shift in the chemical shift towards higher values for all hydrogen atoms from 0.01 to 0.70 ppm. In the case of coniferyl alcohol, this shift is from 0.05 to 0.77 ppm.

The introduction of the second sulfate group into the structure of sulfated derivatives of monolignols also leads to a shift in the chemical shift in the ^{13}C NMR spectra. So for p-coumaril

alcohol, the values for C5 shift from 137.07 to 136.61, for C6 - from 133.63 to 138.28, C3 - from 163.61 to 160.66 ppm. For coniferyl alcohol, the values shift for C3 from 153.52 to 148.25, for C6 - from 133.20 to 139.32, for C5 - from 114.89 to 117.29 ppm.

The chemical shift for sulfated derivatives of coniferyl alcohol is in the range 114.89-158.99 ppm refers to vibrations of carbon in the aromatic ring, and in the range 55.57-73.11 ppm refers to the vibrations of the –CH$_3$ group, chemical shifts are also observed in the region 125.24-139.44 ppm, which can be attributed to the aliphatic part of sulfated derivatives of coniferyl alcohol. [41-43]
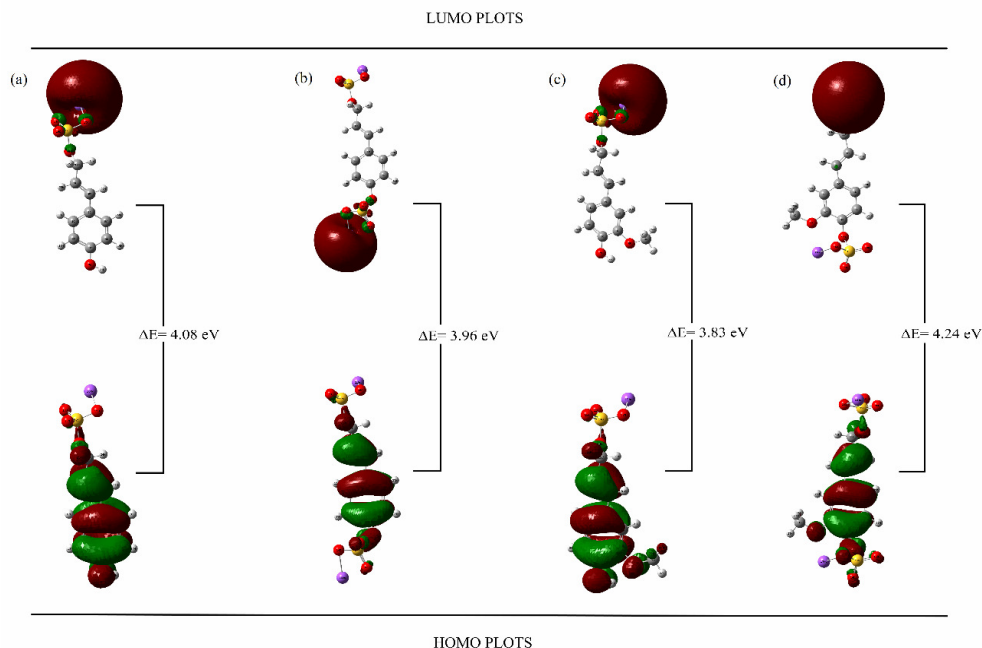

Figure 6: Molecular orbital energy levels of (a) sodium (E)-3-(4-hydroxy-3-methoxyphenyl)allyl sulfate, (b) sodium (E)-2-methoxy-4-(3-(sulfonatooxy)prop-1-en-1-yl)phenyl sulfate, (c) sodium (E)-3-(4-hydroxy-3-methoxyphenyl)allyl sulfate and (d) sodium (E)-2-methoxy-4-(3-(sulfonatooxy)prop-1-en-1-yl)phenyl sulfate

HOMO-LUMO analysis and global electronic description

LUMO (as an electron acceptor) is used to denote the lowest unoccupied molecular orbital, while HOMO (as an electron donor) is used to denote the highest occupied molecular orbital. HOMO and LUMO 3D plots for sulfated coniferyl and p-coumaril alcohols are shown in Figure 6. Electron affinity (A), electronegativity (χ), chemical hardness (η), chemical potential (μo), ionization potential (I) and electrophilicity

index (ω) were calculated using the energy gap between HOMO and LUMO (Table 4).

With a small energy gap between HOMO and LUMO, a molecule can be associated with high polarizability and chemical reactivity, and also low kinetic stability.[44] In sodium (E)-3-(4-hydroxy-3-methoxyphenyl) allyl sulfate, sodium (E)-2-methoxy-4-(3-(sulfonatooxy)prop-1-en-1-yl) phenyl sulfate, sodium (E)-3-(4-hydroxy-3-methoxyphenyl) allyl sulfate and sodium (E)-2-methoxy-4-(3-(sulfonatooxy)prop-1-en-1-yl)

phenyl sulfate, the HOMO-LUMO gap was 4.08, 3.96, 3.83 and 4.24 eV, respectively, demonstrating that charge transfer is observed to a greater extent in sodium (E)-3-(4-hydroxy-3-methoxyphenyl) allyl sulfate.

With the introduction of an additional sulfate group into the structure of sulfated monolignols,

an increase in the value of electronegativity, electron affinity, ionization energy, maximum charge transfer index and electrophilicity index is observed, as well as a decrease in the value of chemical hardness and chemical potential (Table 4).

Table 4

Some electronic parameters of (a) sodium (E)-3-(4-hydroxy-3-methoxyphenyl)allyl sulfate, (b) sodium (E)-2-methoxy-4-(3-(sulfonatooxy)prop-1-en-1-yl)phenyl sulfate, (c) sodium (E)-3-(4-hydroxy-3-methoxyphenyl)allyl sulfate and (d) sodium (E)-2-methoxy-4-(3-(sulfonatooxy)prop-1-en-1-yl)phenyl sulfate

Parameters (eV)	a	b	c	d
E_{HOMO}	-5.9094	-5.9141	-5.6640	-6.1154
E_{LUMO}	-1.8253	-1.9513	-1.8291	-1.8686
Energy band gap (ΔE)	4.0841	3.9628	3.8349	4.2468
Electronegativity(χ)	3.8673	3.9327	3.7465	3.9920
Softness (ς)	0.48	0.5046	0.5215	0.4709
Electron affinity (A)	1.8253	1.9513	1.8291	1.8686
Ionization energy (I)	5.9094	5.9141	5.6640	6.1154
Chemical potential (μ)	-3.8673	-3.9327	-3.7465	-3.9920
Chemical hardness (η)	2.0420	1.9814	1.9174	2.1234
Electrophilicity index (ω)	3.6620	3.9028	3.6601	3.7524
Maximum charge transfer index ($\Delta N max$)	1.8938	1.9848	1.9539	1.8800

Mulliken atomic charges

Mulliken atomic charges of sulfated monolignols were calculated using B3LYP/6-311+G (d, p). The atomic charges of each sulfated monolignol (obtained from the analysis of the Mulliken population) are listed in Table 5. Mulliken atomic charges are related to the vibrational properties of the molecule, and also affect molecular polarizability, atomic charge effect, various aspects of the electronic structure and many properties of molecular systems.[45]

The introduction of an additional sulfate group into the structure of sulfated monolignols leads to a change in Mulliken atomic charges for almost all atoms. Thus, the atomic charges of p-coumarin

alcohol disulfate (in comparison with p-coumarin alcohol monosulfate) have lower values for 1C (-0.7824e), 4C (-0.2780e), 6C (0.8350e), as well as higher values are observed in 2C (-0.2266e), 3C (-0.2450e), 5C (-0.0147e). In the case of the introduction of an additional sulfate group into the structure of coniferyl alcohol monosulfate, a decrease in charges is observed at 1C (up to -0.7733e), 2C (up to -0.3493e), 4C (up to -0.7218e), 6C (up to 1.0082), charges increase at 3C (up to -0.4714e), 5C (up to 0.4738e), 7O (up to -0.1471e). It should be noted the introduction of an additional sulfate group does not significantly affect the charges of Na and H atoms in all samples of sulfated monolignols.

Table 5

Mulliken atomic charges of (a) sodium (E)-3-(4-hydroxy-3-methoxyphenyl)allyl sulfate, (b) sodium (E)-2-methoxy-4-(3-(sulfonatooxy)prop-1-en-1-yl)phenyl sulfate, (c) sodium (E)-3-(4-hydroxy-3-methoxyphenyl)allyl sulfate and (d) sodium (E)-2-methoxy-4-(3-(sulfonatooxy)prop-1-en-1-yl)phenyl sulfate

a		b		c		d	
Atoms	Charges	Atoms	Charges	Atoms	Charges	Atoms	Charges
1C	-0.3561	1C	-0.7824	1C	-0.4911	1C	-0.7733
2C	-0.4756	2C	-0.2266	2C	-0.2038	2C	-0.3493
3C	-0.5662	3C	-0.2450	3C	-0.5052	3C	-0.4714
4C	0.0906	4C	-0.2780	4C	-0.6443	4C	-0.7218
5C	-0.4457	5C	-0.0147	5C	0.4629	5C	0.4738
6C	1.3335	6C	0.8350	6C	1.0777	6C	1.0082

7O	-0.2426	7C	0.0616	7O	-0.3242	7O	-0.1471
8C	-0.0932	8C	-0.0336	8O	-0.2836	8C	-0.2557
9C	0.1981	9C	-0.5041	9C	-0.2158	9C	0.1858
10C	-0.7251	10O	-0.1409	10C	0.5089	10C	-0.0138
11O	-0.0771	11S	0.4262	11C	-0.4040	11C	-0.4247
12S	0.4486	12O	-0.1135	12C	-0.8717	12O	-0.1513
13O	-0.2969	13O	-0.3359	13O	-0.1537	13S	0.4155
14O	-0.3365	14O	-0.6261	14S	0.5509	14O	-0.1052
15O	-0.6449	15Na	0.8788	15O	-0.4625	15O	-0.3359
16Na	0.8723	16O	-0.0696	16O	-0.3102	16O	-0.6320
17H	0.1173	17S	0.4596	17O	-0.4718	17Na	0.8773
18H	0.1272	18O	-0.2993	18Na	0.8182	18O	-0.0681
19H	0.1025	19O	-0.3399	19H	0.1424	19S	0.4579
20H	0.1213	20O	-0.6451	20H	0.1463	20O	-0.2986
21H	0.2457	21Na	0.8712	21H	0.1519	21O	-0.3383
22H	0.1228	22H	0.1037	22H	0.3061	22O	-0.6453
23H	0.1286	23H	0.1753	23H	0.1724	23Na	0.8717
24H	0.1860	24H	0.1258	24H	0.1617	24H	0.0977
25H	0.1653	25H	0.1200	25H	0.1619	25H	0.1754
		26H	0.1220	26H	0.1425	26H	0.1360
		27H	0.1262	27H	0.1516	27H	0.1584
		28H	0.1862	28H	0.1837	28H	0.1412
		29H	0.1633	29H	0.2029	29H	0.1382
						30H	0.1183
						31H	0.1267
						32H	0.1856
						33H	0.1638

Molecular electrostatic potential (MEP) analysis

In order to assess the regions of nucleophilic and electrophilic attacks and interactions of hydrogen bonds in sulfated monolignols, their maps of molecular electrostatic potential (MEP) were studied (Fig. 7).[32] Different electrostatic potential values give different colors on the surfaces of the molecular electrostatic potential.

The negative region of the MEP is shown in yellow and is associated with electrophilic capacity, including hydroxyl groups and sulfate groups.
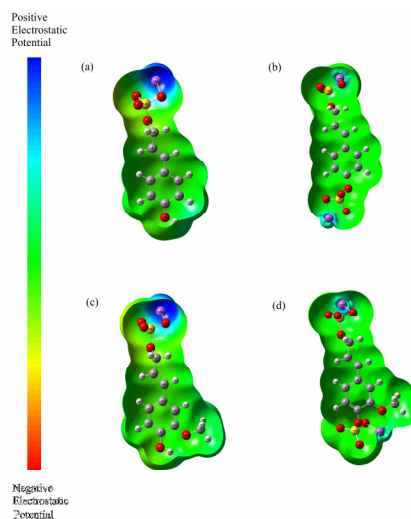

Figure 7: Molecular electrostatic potential surfaces of (a) sodium (E)-3-(4-hydroxy-3-methoxyphenyl)allyl sulfate, (b) sodium (E)-2-methoxy-4-(3-(sulfonatooxy)prop-1-en-1-yl)phenyl sulfate, (c) sodium (E)-3-(4-hydroxy-3-methoxyphenyl)allyl sulfate and (d) sodium (E)-2-methoxy-4-(3-(sulfonatooxy)prop-1-en-1-yl)phenyl sulfate

The positive area is marked in blue, which is associated with nucleophilic ability of sodium atoms.[32] The highest electronegativity of sulfate groups leads to their highest reactivity in sulfated monolignols. A negative electrostatic potential is located around oxygen atoms, and a positive electrostatic potential is localized on the rest of the sulfated monolignols.

CONCLUSION

This article presents the results of a theoretical study of sulfated monolignols (p-coumaril, coniferyl alcohols). The molecular geometry of sulfated monolignols is investigated by the density functional theory (DFT/B3LYP) method, with 6-311+G (d, p) basis set. The obtained theoretical IR spectra are in good agreement with the experimental data presented in the literature. According to the study of theoretical ^{13}C NMR spectra, it was shown that the introduction of an additional sulfate group into monosubstituted sulfates of monolignols displaces the chemical shift towards larger values. Based on the HOMO-LUMO analysis, it was shown that the energy gap with the lowest value corresponds to the monosulfated coniferyl alcohol. The obtained data can help researchers in more accurate identification of lignin sulfation products, monolignols and their derivatives. Thus, the theoretical IR and NMR spectra obtained in this work can help researchers towards a more detailed understanding of the mechanism of lignin sulfation, especially if it is carried out with new sulfating agents. The position of the sulfate group (and, consequently, the mechanism of sulfation) has a significant effect on the biological activity of polymers.[46,47]

In different sources of raw materials, the ratio of monolignols varies significantly. As a result, the content of aliphatic and phenolic hydroxyl groups that can be substituted using reagents changes. Thus, for controlled sulfation processes and competent selection of reagents for industrial valorization of lignins to obtain functional derivatives, it is necessary to understand the mechanisms of selective sulfation based on the DFT method. Based on the data obtained, a cost-effective selection of sulphating reagent–lignin pairs is possible (depending on the source and method of lignin isolation).

REFERENCES

[1] F. G. Calvo-Flores (Ed.), "Lignin and Lignans as Renewable Raw Materials: Chemistry, Technology and Applications", Wiley, 2015, pp. 4-7, https://www.wiley.com/en-us/Lignin+and+Lignans+as+Renewable+Raw+Materials%3A+Chemistry%2C+Technology+and+Applications-p-9781118597866

[2] P. Wool and X. S. Sun (Eds.), "Bio-based Polymers and Composites", London, Elsevier Academic Press, 2005, 640 p., https://www.elsevier.com/books/bio-based-polymers-and-composites/wool/978-0-12-763952-9

[3] C. Heitner, D. Dimmel and J. Schmidt (Eds.), "Lignin and Lignans: Advances in Chemistry", CRC Press, Taylor and Francis Group, 2010, 683 p., https://doi.org/10.1201/EBK1574444865

[4] P. Bajpai (Ed.), "Recent Developments in Cleaner Production. Environmentally Friendly Production of Pulp and Paper", Hoboken, NJ, USA, John Wiley & Sons, Inc. 2010, p. 264-340, https://www.wiley.com/en-us/Environmentally+Friendly+Production+of+Pulp+and+Paper-p-9780470528105

[5] B. N. Kuznetsov, Y. N. Malyar, S. A. Kuznetsova, L. I. Grishechko, A. S. Kazachenko *et al.*, *J. Sib. Fed. Univ. Chem.*, **4**, 454 (2016), https://doi.org/10.17516/1998-2836-2016-9-4-454-482

[6] I. L. Deineko, *Chem. Plant Raw Mater.*, **1**, 5 (2003)

[7] M. J. Torre, A. Moral, M. D. Hernández, E. Cabeza and A. Tijero, *Ind. Crop. Prod.*, **45**, 58 (2013), https://doi.org/10.1016/j.indcrop.2012.12.002

[8] V. V. Simonova, T. G. Shendrik and B. N. Kuznetsov, *J. Sib. Fed. Univ. Chem.*, **4**, 340 (2010)

[9] A. Agrawal, N. Kaushik and S. Biswas, *The sciTech J.*, **1**, 30 (2014)

[10] A. Raghuraman, V. Tiwari, Q. Zhao, D. Shukla, A. K. Debnath *et al.*, *Biomacromolecules*, **8**, 1759 (2007), https://doi.org/10.1021/bm0701651

[11] B. L. Henry and U. R. Desai, *Thromb. Res.*, **134**, 1123 (2014), https://doi.org/10.1016/j.thromres.2014.08.024

[12] V. V. Leonov, E. Yu. Fursova and A. I. Galochkin, *Bull. Ugra St. Univ.*, **3**, 78 (2006)

[13] Yu. N. Malyar, N. Yu. Vasil'yeva, A. S. Kazachenko, G. P. Skvortsova, I. V. Korol'kova *et al.*, *Chem. Raw Plant Mat.*, **3**, 5 (2020), https://doi.org/10.14258/jcprm.2020036931

[14] B. N. Kuznetsov, N. Yu. Vasilyeva, A. S. Kazachenko, G. P. Skvortsova, V. A. Levdansky *et al.*, *J. Sib. Fed. Univ. Chem.*, **11**, 122 (2018), https://doi.org/10.17516/1998-2836-0063

[15] V. A. Levdansky, N. Y. Vasilyeva, Y. N. Malyar, A. V. Levdansky, A. A. Kondrasenko *et al.*, *Biomass Conv. Bioref.*, (2020), https://doi.org/10.1007/s13399-020-00706-0

[16] B. N. Kuznetsov, N. Yu. Vasilyeva, A. S. Kazachenko, V. A. Levdansky, A. A. Kondrasenko *et al.*, *Wood Sci. Technol.*, **54**, 365 (2020), https://doi.org/10.1007/s00226-020-01157-6

[17] P. Prinsen, A. Narani, A. F. Hartog, R. Wever and G. Rothenberg, *ChemSusChem*, **10**, 2267 (2017)

[18] V. Profant, C. Johannessen, E. W. Blanch, P. Bour and V. Baumruk, *Phys. Chem. Chem. Phys.*, **21**, 7367 (2019), https://doi.org/10.1039/C9CP00472F

[19] F. Akman, A. S. Kazachenko, N. Yu. Vasilyeva and Yu. N. Malyar, *J. Mol. Struct.*, (2020), https://doi.org/10.1016/j.molstruc.2020.127899

[20] T. R. Rudd, M. A. Skidmore, S. E. Guimond, C. Cosentino, G. Torri *et al.*, *Glycobiology*, **19**, 52 (2009), https://doi.org/10.1093/glycob/cwn103

[21] K. Matsuo, H. Namatame, M. Taniguchi and K. Gekko, *Biosci. Biotechnol. Biochem.*, **73**, 557 (2009), https://doi.org/10.1271/bbb.80605

[22] N. Mainreck, S. Brézillon, G. D. Sockalingum, F. X. Maquart, M. Manfait *et al.*, *J. Pharm. Sci.*, **100**, 441 (2011), https://doi.org/10.1002/jps.22288

[23] W. Garnjanagoonchorn, L. Wongekalak and A. Engkagul, *Chem. Eng. Process Process Intensif.*, **46**, 465 (2007)

[24] A. S. Kazachenko, F. N. Tomilin, A. A. Pozdnyakova, N. Y. Vasilyeva, Y. N. Malyar *et al.*, *Chem. Pap.*, **74**, 4103 (2020), https://doi.org/10.1007/s11696-020-01220-3

[25] A. Rüther, A. Forget, A. Roy, C. Carballo, F. Mießmer *et al.*, *Angew. Chem.*, **129**, 4674 (2017), https://doi.org/10.1002/ange.201701019

[26] N. R. Yaffe, A. Almond and E. W. Blanch, *J. Am. Chem. Soc.*, **132**, 10654 (2010), https://doi.org/10.1021/ja104077n

[27] A. Canales, I. Boos, L. Perkams, L. Karst, T. Luber *et al.*, *Angew. Chem. Int. Ed.*, **56**, 14987 (2017), https://doi.org/10.1002/anie.201709130

[28] T. Klepach, H. Zhao, X. Hu, W. Zhang, R. Stenutz *et al.*, *Met. Mol. Biol.*, **1273**, 289 (2015), https://doi.org/10.1007/978-1-4939-2343-4_20

[29] A. G. Gerbst, A. V. Nikolaev, D. V. Yashunsky, A. S. Shashkov, A. S. Dmitrenok *et al.*, *Sci. Rep.*, **7**, 8934 (2017), https://doi.org/10.1038/s41598-017-09055-x

[30] O. E. Shklyaev, J. D. Kubicki, H. D. Watts and V. H. Crespi, *Cellulose*, **21**, 3979 (2014), https://doi.org/10.1007/s10570-014-0448-3

[31] F. Akman, *Can. J. Phys.*, **94**, 583 (2016), https://doi.org/10.1139/cjp-2016-0041

[32] F. Akman, *Cellulose Chem. Technol.*, **53**, 243 (2019), https://doi.org/10.35812/CelluloseChemTechnol.2019.53.24

[33] F. Akman, *J. Therm. Comp. Mater.*, **31**, 729 (2017), https://doi.org/10.1177/0892705717720253

[34] T. T. V. Tran, B. T. Huy, H. B. Truong, M. L. Bui, T. T. T. Thanh *et al.*, *Monatsh Chem.*, **149**, 197 (2018), https://doi.org/10.1007/s00706-017-2056-z

[35] S. Barsberg, *J. Phys. Chem. B.*, **114**, 11703 (2010), https://doi.org/10.1021/jp104213z

[36] F. Akman, *Polym. Bull.*, **74**, 2975 (2017), https://doi.org/10.1007/s00289-016-1875-0

[37] M. J. Frisch, G. W. Trucks, H. B. Schlegel, G. E. Scuseria, M. A. Robb *et al.*, Gaussian 09, Revision C.01, Gaussian, Inc., Wallingford CT, 2009

[38] R. Dennington, T. Keith and J. Millam, GaussView, Version 5, Semichem Inc., Shawnee Mission KS, 2010

[39] A. D. Becke, *Phys. Rev. A*, **38**, 3098 (1988)

[40] C. Lee, W. Yang and R. G. Parr, *Phys. Rev. B*, **37**, 785 (1988)

[41] W. A. Wood and S. T. Kellogg (Eds.), "Characterization of Lignin by 1H and 13C NMR Spectroscopy", San Diego, CA, Academic Press, 1988, pp. 137-174

[42] C. W. Dence (Ed.), "Carbon 13 Nuclear Magnetic Resonance Spectroscopy", New York, Springer☐Verlag, 1992. pp. 250-273

[43] L. V. Kanitskaya, I. D. Kalikhman, S. A. Medvedeva, I. A. Belousova, V. A. Babkin *et al.*, *Khim. Drev.*, **4**, 73 (1992)

[44] I. Fleming, "Frontier Orbital and Organic Chemical Reactions", New York, John Wiley and Sons, 1976, https://doi.org/10.1002/prac.19783200525

[45] R. S. Mulliken, *J. Chem. Phys.*, **23**, 1833 (1955)

[46] H. E. Caputo, J. E. Straub and M. W. Grinstaff, *Chem. Soc. Rev.*, **48**, 2338 (2019), https://doi.org/10.1039/c7cs00593h

[47] N. N. Drozd, S. A. Kuznetsova, Yu. N. Malyar, N. Yu. Vasilyeva and B. N. Kuznetsov, *Bull. Exp. Biol. Med.*, **169**, 815 (2020), https://doi.org/10.1007/s10517-020-04987-3